Delft University of Technology

Speed and heading control-based collision avoidance for a ship towing system

Zhang, Lei; Liu, Wenjie; Du, Zhe; Du, Lei; Li, Xiaobin

DOI
10.1016/j.isatra.2022.10.010

Publication date
2023

Document Version
Final published version

Published in
ISA Transactions

Citation (APA)
Zhang, L., Liu, W., Du, Z., Du, L., & Li, X. (2023). Speed and heading control-based collision avoidance for a ship towing system. *ISA Transactions*, *135*, 52-65. https://doi.org/10.1016/j.isatra.2022.10.010

Important note
To cite this publication, please use the final published version (if applicable).
Please check the document version above.

Copyright
Other than for strictly personal use, it is not permitted to download, forward or distribute the text or part of it, without the consent of the author(s) and/or copyright holder(s), unless the work is under an open content license such as Creative Commons.

Takedown policy
Please contact us and provide details if you believe this document breaches copyrights.
We will remove access to the work immediately and investigate your claim.

This work is downloaded from Delft University of Technology.
For technical reasons the number of authors shown on this cover page is limited to a maximum of 10.

ISA Transactions 135 (2023) 52–65

Contents lists available at ScienceDirect

ISA Transactions

journal homepage: www.elsevier.com/locate/isatrans

Research article

Speed and heading control-based collision avoidance for a ship towing system

Lei Zhang [a,b], Wenjie Liu [b], Zhe Du [c,*], Lei Du [b], Xiaobin Li [a]

[a] Wuhan University of Technology, School of Naval Architecture, Ocean and Energy Power Engineering, Wuhan, China
[b] Wuhan University of Technology, School of Navigation, Wuhan, China
[c] Department of Maritime and Transport Technology, Delft University of Technology, Mekelweg 2, 2628 CD, Delft, The Netherlands

ARTICLE INFO

Article history:
Received 23 April 2022
Received in revised form 6 October 2022
Accepted 14 October 2022
Available online 23 October 2022

Keywords:
Ship towing system
Collision avoidance
Model predictive control
Conflict resolution

ABSTRACT

Collision avoidance is a priority task for ensuring the safety of a maritime transportation system. However, for a ship towing system, which is characterized by multiple vessels and physical connections, the research works about collision avoidance is limited. Thus, this paper proposes a speed and heading control-based conflict resolution of a ship towing system for collision avoidance. Two systems compose the core of the proposed conflict resolution: the risk assessment system and the coordination control system. The risk assessment is to identify the conflict and determine the time of avoiding action by calculating the index of conflict and the available maneuvering margin. The coordination control is based on the model predictive control (MPC) strategy to cooperatively control two tugboats for regulating the position, heading, and speed of the manipulated ship. Simulation experiments show that according to the index of conflict, the time cost, and the fuel consumption, a selected operation of combined heading and speed can be recommended for a ship towing system to provide a safer and more efficient towage manipulation.
© 2022 The Author(s). Published by Elsevier Ltd on behalf of ISA. This is an open access article under the CC BY license (http://creativecommons.org/licenses/by/4.0/).

1. Introduction

In the maritime field, collision avoidance is a priority task for ensuring the safety of a maritime transportation system during its navigation [1]. It is usually solved by path planning algorithm in the navigation system [2]. However, this issue becomes more challenging and imperative when the maritime transportation system becomes complex and its maneuverability is restricted. One of the typical examples is the towing system. As the development and exploitation of ocean resources becomes frequent, the application of a towing system plays a more critical role in the maritime field, such as drilling platform transportation [3], offshore wind farm deployment [4–6], distressed vessels salvage [7,8], ship escort in ice conditions [9–11], and ship-assisted berthing [12]. Thus, an alternative way should be designed to solve the collision avoidance problem for such a maneuverability-restricted system.

From the perspective of the structure of a maritime transportation system, the most vital components are guidance, navigation, and control systems (GNC systems) [13]. The navigation system is to obtain information about the environment and the states of the maritime transportation system. The guidance system is to provide missions and objectives for the control system according to the data from the navigation system. The control system is to calculate the proper forces and moments for the actuators of the maritime transportation system based on the control objectives. While for collision avoidance problems in the maritime field, there are also three key components: motion prediction, conflict detection, and collision resolution [14]. Motion prediction is to estimate the future trajectories (position and heading) and speeds of the own ship and the obstacles. Conflict detection is to check collision risk and make decisions on whether to take action. Conflict resolution is to find solutions to relieve risk or avoid collisions.

Combining the structure of the GNC system and the component of the collision avoidance problem, it can be seen from Fig. 1 that the solution to the collision avoidance problem involves all three GNC components. The problem of motion prediction is solved through the dynamics model and the information on the states of the own ship and obstacles provided by the navigation system. The problem of conflict detection is tackled by a collision risk assessment mechanism designed in the guidance system. The problem of conflict resolution is addressed through both the guidance and control system, where the guidance system provides control objectives and the control system calculates the corresponding forces and moments.

Thus, for a single vessel system, the general idea of solving the collision avoidance problem is first to plan a collision-free path in the guidance system by path planning algorithms, such

* Corresponding author.
E-mail address: z.du@tudelft.nl (Z. Du).

https://doi.org/10.1016/j.isatra.2022.10.010
0019-0578/© 2022 The Author(s). Published by Elsevier Ltd on behalf of ISA. This is an open access article under the CC BY license (http://creativecommons.org/licenses/by/4.0/).

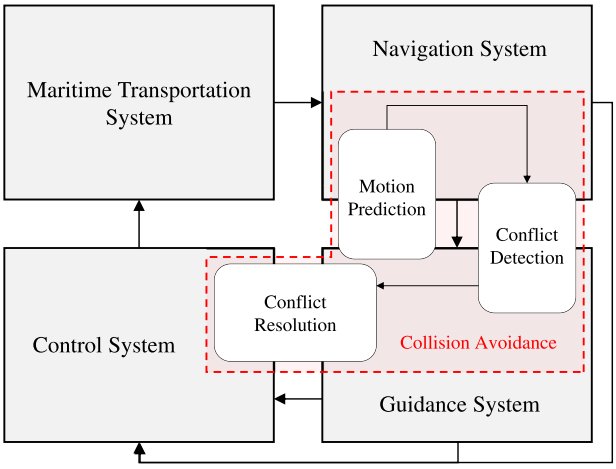

Fig. 1. Distribution of the collision avoidance components in the structure of the GNC system of a maritime transportation system.

as artificial potential field algorithm [15,16], velocity obstacle algorithm [17,18], (improved) A-star algorithm [19–21], etc. The planned path or trajectory is actually a form of data carrying the information of the position and heading of the vessel. Then, the above data is used as the control objectives in the control system to compute control input.

For a multi-vessel cyber-connected system, which is the maritime transportation system in which all vessels are clustered in a certain range maintaining a safe distance and the connection is realized through the networks [22]. Researchers usually cope with collision avoidance problems by first arranging a specific formation to cooperatively control the relative positions of multiple vessels, then keeping or changing this formation to avoid obstacles. While in this process, multi-objective optimization problems are also involved [23]. The typical formation is the triangle shape composed of three vessels [24,25]. For more than three vessels, the reconfigurable formation can be applied [26,27]. Alternatively, a line formation (or a vessel-train formation) is proposed to deal with the collisions in a narrow waterway of port areas [28].

For a towing system, which is characterized by multiple vessels and physical connections, the research works about collision avoidance is limited. Authors in [29] directly use the model predictive control method to regulate the distance between the towing system and the obstacles so that keeps the towing system away from the risks. However, this research mainly focuses on conflict resolution in the control system, there is a lack of rational conflict detection mechanism designed in the guidance system.

Given the above analysis, the primary aim of this work is to propose a novel conflict resolution for collision avoidance problem of a towing system. The contributions of this paper can be summarized in three aspects as follows:

1. Formulate a risk assessment criteria for a towing system based on its velocity and heading to evaluate the collision risk and put forward the risk relief strategy.
2. Propose a MPC-based control method for a towing system to simultaneously regulate its position, heading, and velocities.
3. Provide a recommended collision avoidance operation for a maneuverability-restricted ship towing system by considering the efficiency of risk elimination, the time of path restoration, and the consumption of fuel.

The remainder of this paper is arranged as follows. Section 2 introduces the dynamics model of the ship, tugboats, and their physically connected towing system. Section 3 presents the conflict detection mechanism based on risk assessment. Section 4 proposes the speed and heading control-based towage conflict resolution method. A case study is simulated in Section 5 to demonstrate the feasibility of the proposed method and the applicability of the results. Conclusions and future research directions are given in Section 6.

2. Dynamics model of the towing system

Without loss of generality, we consider a towing system operating in port areas that consists of one manipulated ship and two tugboats, where the ship is set as no power, and the power sources of the towing system are offered by the two tugs. The front tug (Tug 2) is to increase the speed and adjust the heading of the ship, while the aft tug (Tug 1) is to decrease the speed and stabilize the course of the ship.

The plane motion of a vessel can be described by the 3-DOF (degree of freedom) kinematics and kinetics model, which is expressed as [30]:

$$\begin{aligned}&\dot{\boldsymbol{\eta}}(t)=\boldsymbol{R}(\psi(t))\boldsymbol{\nu}(t)\\&\boldsymbol{M}\dot{\boldsymbol{\nu}}(t)+\boldsymbol{C}(\boldsymbol{\nu}(t))\boldsymbol{\nu}(t)+\boldsymbol{D}\boldsymbol{\nu}(t)=\boldsymbol{\tau}(t)+\boldsymbol{\tau}_{\mathrm{e}}(t),\end{aligned}\tag{1}$$

where $\boldsymbol{\eta}(t)=[x(t)\ y(t)\ \psi(t)]^{\mathrm{T}}\in\mathbb{R}^3$ is the position vector in the world frame (North-East-Down) including position coordinates ($x(t)$, $y(t)$) and heading $\psi(t)$; $\boldsymbol{\nu}(t)=[u(t)\ v(t)\ r(t)]^{\mathrm{T}}\in\mathbb{R}^3$ is the velocity vector in the body-fixed frame containing the velocity of surge $u(t)$, sway $v(t)$ and yaw $r(t)$; $\boldsymbol{R}\in\mathbb{R}^{3\times3}$ is the rotation matrix from the body frame to the world frame, which is a function of heading:

$$\boldsymbol{R}(\psi(t))=\begin{bmatrix}\cos(\psi(t)) & -\sin(\psi(t)) & 0\\ \sin(\psi(t)) & \cos(\psi(t)) & 0\\ 0 & 0 & 1\end{bmatrix}.\tag{2}$$

The terms $\boldsymbol{M}\in\mathbb{R}^{3\times3}$, $\boldsymbol{C}\in\mathbb{R}^{3\times3}$ and $\boldsymbol{D}\in\mathbb{R}^{3\times3}$ are the mass (inertia), Coriolis-centripetal and damping matrix, respectively. The first two matrices include rigid-body and added mass parts, and the last matrix is only considered to have a linear part. The variable $\boldsymbol{\tau}(t)=[\tau_{\mathrm{u}}(t)\ \tau_{\mathrm{v}}(t)\ \tau_{\mathrm{r}}(t)]^{\mathrm{T}}\in\mathbb{R}^3$ is the controllable input referring to the forces $\tau_{\mathrm{u}}(t)$, $\tau_{\mathrm{v}}(t)$ and moment $\tau_{\mathrm{r}}(t)$, while $\boldsymbol{\tau}_{\mathrm{e}}(t)\in\mathbb{R}^3$ stands for the environmental disturbance forces and moment. Considering the wind effect is dominant in the port areas, the environmental disturbances are divided into the wind effect $\boldsymbol{\tau}_{\mathrm{w}}(t)\in\mathbb{R}^3$ and the other unknown effects $\boldsymbol{\tau}_{\mathrm{cw}}(t)\in\mathbb{R}^3$ (mainly refer to waves and currents):

$$\boldsymbol{\tau}_{\mathrm{e}}(t)=\boldsymbol{\tau}_{\mathrm{w}}(t)+\boldsymbol{\tau}_{\mathrm{cw}}(t).\tag{3}$$

As seen the ship in Fig. 2, the controllable input of the ship $\boldsymbol{\tau}_{\mathrm{S}}(t)$ (in (1), $\boldsymbol{\tau}(t)\triangleq\boldsymbol{\tau}_{\mathrm{S}}(t)$) can be expressed as:

$$\boldsymbol{\tau}_{\mathrm{S}}(t)=\sum_{i=1}^{2}\boldsymbol{\tau}_{\mathrm{S}i}(t)=\sum_{i=1}^{2}\boldsymbol{B}_{\mathrm{S}i}(t)F_i(t),\tag{4}$$

where $\boldsymbol{\tau}_{\mathrm{S}i}(t)$ represents the towing forces and moment of the tug i; $F_i(t)$ is the towing force from the tug i through the towline; $\boldsymbol{B}_{\mathrm{S}i}(t)\in\mathbb{R}^3$ is the configuration matrix with respect to the object-body frame, it is a function of the towing angle $\alpha_i(t)$ expressed as:

$$\boldsymbol{B}_{\mathrm{S}1}(t)=-\begin{bmatrix}\cos(\alpha_1(t))\\ \sin(\alpha_1(t))\\ l_1\sin(\alpha_1(t))\end{bmatrix}\quad\boldsymbol{B}_{\mathrm{S}2}(t)=\begin{bmatrix}\cos(\alpha_2(t))\\ \sin(\alpha_2(t))\\ l_2\sin(\alpha_2(t))\end{bmatrix},\tag{5}$$

where l_1 and l_2 are the distance from the center of gravity of the ship to its stern and bow, respectively.

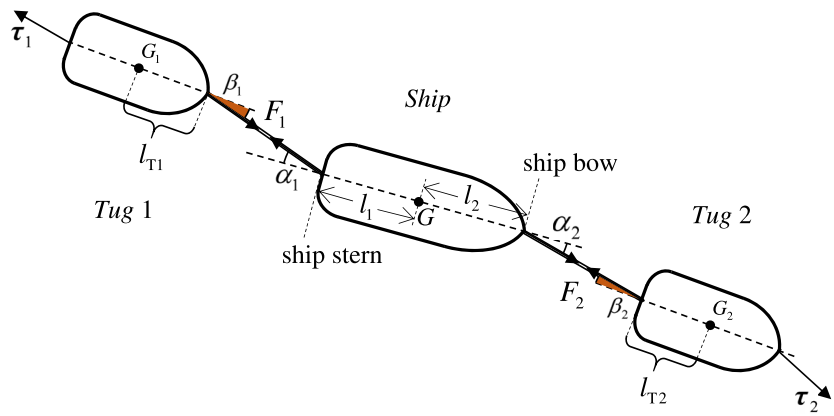

Fig. 2. Forces on the three vessels in the towing system.

As seen the two tugboats in Fig. 2, the controllable input of the two tugboats (in (1), $\boldsymbol{\tau}(t) \triangleq \boldsymbol{\tau}_i(t)\ \ (i = 1, 2)$) can be expressed as:

$$\boldsymbol{\tau}_i(t) = \boldsymbol{\tau}_{\mathrm{T}i}(t) + \boldsymbol{\tau}_{\mathrm{F}i}(t), \tag{6}$$

where $\boldsymbol{\tau}_{\mathrm{T}i}(t) \in \mathbb{R}^3$ denotes the thruster forces and moment of the tug i; $\boldsymbol{\tau}_{\mathrm{F}i}(t) \in \mathbb{R}^3$ is the forces and moment to compensate for the reaction of towing force, which can be expressed as:

$$\boldsymbol{\tau}_{\mathrm{F}i}(t) = \boldsymbol{B}_{\mathrm{T}i}(t) F_i(t), \tag{7}$$

where $\boldsymbol{B}_{\mathrm{T}i}(t) \in \mathbb{R}^3$ is the configuration matrix with respect to the tug-body frame, which is a function of the tug angle $\beta_i(t)$:

$$\boldsymbol{B}_{\mathrm{T}1}(t) = \begin{bmatrix} \cos(\beta_1(t)) \\ \sin(\beta_1(t)) \\ l_{\mathrm{T}1} \sin(\beta_1(t)) \end{bmatrix} \quad \boldsymbol{B}_{\mathrm{T}2}(t) = -\begin{bmatrix} \cos(\beta_2(t)) \\ \sin(\beta_2(t)) \\ l_{\mathrm{T}2} \sin(\beta_2(t)) \end{bmatrix}, \tag{8}$$

where $l_{\mathrm{T}1}$ is the distance from the center of gravity of the Tug 1 to its bow; $l_{\mathrm{T}2}$ is the distance from the center of gravity of the Tug 2 to its stern.

From (4) to (8), it can be noticed that the interconnection between the ship system and the tug system is the towing force $F_i(t)$. For the ship, the towing force provides power to move it, while for tugs, the towing force is the resistance effect which needs to be compensated.

3. Risk assessment-based conflict detection

3.1. Conflict identification

To consider the dynamic nature of ship maneuvers during collision avoidance, Non-Linear Velocity Obstacle (NLVO) algorithm is adopted for conflict identification [31]. By utilizing the NLVO algorithm, the spatiotemporal relationship between a ship pair is projected into one ship's velocity domain, see Fig. 3. An elliptical ship domain is employed, and the prohibited area around this towing system includes the elliptic ship domain around each ship in this towing system and the area around the towline connecting the tug and the assisted ship:

$$S_{\mathrm{NL_VO}}(k) = \bigcup_{t,*} \left(\frac{P_{\mathrm{TS}_*}(x_*, y_*, t) - P_{\mathrm{Intr}}(x, y, k)}{(t-k)} \right) \oplus \frac{\mathrm{Conf}P(O_{*,t}, R_*)}{(t-k)}, \tag{9}$$

where $S_{\mathrm{NL_VO}}(k)$ is velocity obstacle zone at time instant k marked in light red in Fig. 3(b), which is the collection of all conflicting velocities of the target ship that leading to collision with this towing system. The term $\mathrm{P}_{\mathrm{TS}_*}(x_*, y_*, t)$ represents the trajectory of each vessel in the towing system ($*$ stands for S or i, $(i = 1, 2)$); $P_{\mathrm{Intr}}(x, y, k)$ is the position of the intruder vessel. $\mathrm{Conf}P(O_{*,t}, R_j)$ is the prohibited area around this towing system, shown in Fig. 3(a), where O is the location of each vessel, R is the size of the elliptic ship domain around each vessel.

A collision is projected to occur if the another ship's velocity falls into the velocity obstacle of this towing system ($S_{\mathrm{NL_VO}}$):

$$IC(t) = \begin{cases} 1, & \text{if } V_{\mathrm{TS}}(t) \cap S_{\mathrm{NL_VO}}(t) \neq \emptyset \\ 0, & \text{else}, \end{cases} \tag{10}$$

where V_{TS} is the velocity of the target ship (TS). In Fig. 3(b), the dashed ellipse in red indicates the velocity obstacle zone of the towed ship in a certain position, and the dashed ellipse in blue and green presents the velocity obstacle zone of each tugboat in a certain position respectively. The area marked in deep red is the conflicting velocity set of this towing system in a certain position. The collision risk exists for V_{TS1}, while there is no collision risk for V_{TS2}.

3.2. Action timing determination

The timing of a vessel taking evasive maneuvers is primarily affected by the risk perceived by the navigator [32]. The available maneuvering margin *AMM* is selected as a proxy to reflect the risk perceived by the navigator [33]. It is measured based on the proportion of maneuvers of all the available maneuvers by which a vessel can eliminate potential conflicts. So the *AMM* can be expressed as:

$$AMM(t) = \frac{\sum \delta_{\mathrm{s}}(t)}{\delta_{\mathrm{a}}(t)}, \quad \text{if } \exists V(t) \in RV(\delta_{\mathrm{s}}(t)) : \ V(t) \cap S_{\mathrm{NL_VO}}(t) = \emptyset \tag{11}$$

where $\delta_{\mathrm{s}}(t)$ is the adopted rudder angle that can eliminate the existing conflict; $\delta_{\mathrm{a}}(t)$ is all the available rudder angles of a ship; *RV* is the own ship's reachable velocity after steering with a demanded rudder angle.

When determining the action timing of a towing system, we made the following assumptions. Due to restricted maneuverability and the distinctiveness of the assisted ship, the towing system has the priority to use the fairway, which is consistent with the practical scenario. The towing systems is required to maneuver to prevent the risk severity becoming serious. Here, when the $AMM(t)$ of an intruder below its low threshold ($AMM_{\min}$), which is set as 0.4 based on our previous work [34], the towing system needs to maneuver for safe passing.

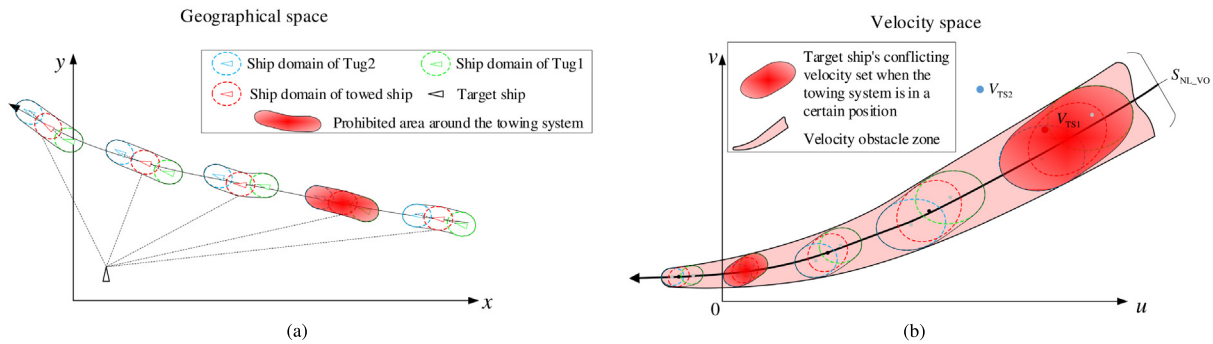

Fig. 3. Ship conflict identification based on NLVO algorithm. (For interpretation of the references to color in this figure legend, the reader is referred to the web version of this article.)

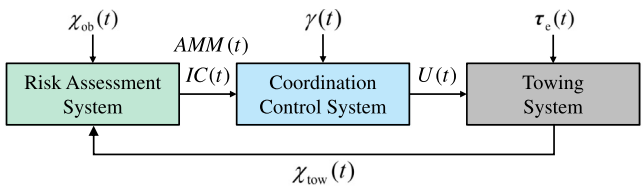

Fig. 4. System structure of the collision resolution in the towage operation.

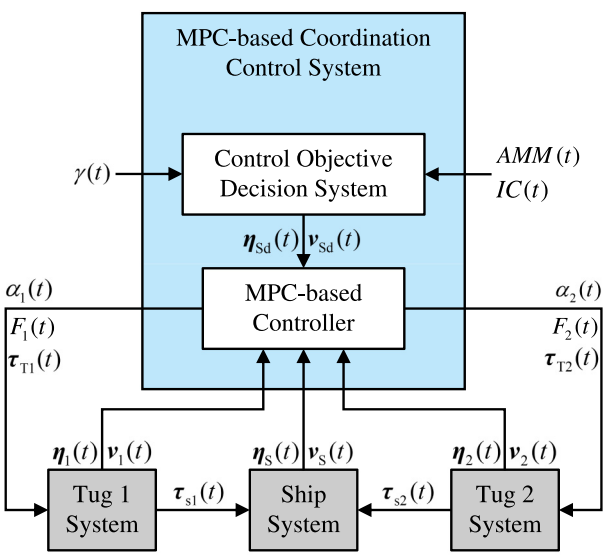

Fig. 5. Diagram of the coordination control system.

4. Coordination control-based collision resolution

Based on the system model and risk assessment mechanism, the collision resolution for a towing system can be put forward.

As shown in Fig. 4, the collision resolution is implemented by consisting of two main systems: the risk assessment system and the coordination control system. The risk assessment system first uses the current and future states of the obstacle ($\chi_{ob}(t)$) and the towing system ($\chi_{tow}(t)$) to calculate the index of conflict $IC(t)$ and the available maneuvering margin $AMM(t)$. Based on the calculated $IC(t)$, $AMM(t)$, and the potential control objectives $\gamma(t)$, the coordination control system then computes the control inputs $U(t)$ to the towing system. Finally, under the environmental disturbances $\boldsymbol{\tau}_e(t)$, the towing system takes avoidance action according to the control inputs.

The risk assessment system has been elaborated in Section 3, so this section focuses on the coordination control system. Since the towing system is restricted in maneuverability which requires more time to respond to the control orders, and the control inputs and control constraints are multiple, it is necessary to use an optimization-based predictive control strategy to regulate this system and achieve collision avoidance. Thus, the Model Predictive Control (MPC) is applied in this work.

The diagram of the MPC-based coordination control system is shown in Fig. 5. It is seen that the control system contains two modules: the control objective decision system and the MPC-based controller. The first module is to decide the current control objectives $\boldsymbol{\eta}_{Sd}(t)$, $\boldsymbol{\nu}_{Sd}(t)$ according to $AMM(t)$, $IC(t)$, and $\gamma(t)$. Based on the calculated control objectives and the current position and velocity of the ship and two tugboats, the MPC-based controller computes the towing angle ($\alpha_i(t)$), towing force ($F_i(t)$), and thrust forces and moment ($\boldsymbol{\tau}_{Ti}(t)$) for two tugboats. Finally, the two tug systems provide towing forces and moment $\boldsymbol{\tau}_{si}$ to the manipulated ship.

4.1. Control objective decision system

In this system, the control objectives are determined by whether the towing system should take avoiding actions. According to (10), if $IC(t) = 0$, meaning that there is no collision risk and the towing system does not need to take avoiding actions. So the control objectives are the position and heading of the waypoint:

$$\eta_{Sd} = \begin{bmatrix} x_{Wj} \\ y_{Wj} \\ \psi_{Wj} \end{bmatrix} \quad \nu_{Sd} = \begin{bmatrix} 0 \\ 0 \\ 0 \end{bmatrix}, \tag{12}$$

where (x_{Wj}, y_{Wj}) and ψ_{Wj} are the position and heading of the waypoint j, respectively.

If $IC(t) = 1$, although the collision risk exists, the towing system still needs to check whether the value of $AMM(t)$ is smaller than its low threshold AMM_{min}. If $AMM(t) \le AMM_{min}$, the towing system has to take avoiding actions, and the control objectives are the reachable speed and heading:

$$\eta_{Sd} = \begin{bmatrix} x_{Wj} \\ y_{Wj} \\ \psi_{Sd} \end{bmatrix} \quad \nu_{Sd} = \begin{bmatrix} u_{Sd} \\ 0 \\ 0 \end{bmatrix}, \tag{13}$$

where ψ_{Sd} and u_{Sd} are the reachable heading and surge speed of the ship.

The time of path returning for the towing system is determined by the variable $IC(t)$ and the distance between the towing system and the obstacles. When $IC(t) = 0$, it can only mean that the collision risk is eliminated under the current speed and heading of the towing system. So the towing system should still maintain the speed and heading calculated in (13) a period of

time until the distance between the towing system and the obstacles does not reduce more. After this point, the towing system can return to the original path.

The control objective decision mechanism is summarized in **Algorithm 1** (at the time instant k).

Algorithm 1 Control Objective Decision Mechanism

Input: Maneuvering margin $AMM(k)$; Index of conflict $IC(k)$; Potential control objectives $\gamma(k)$; Flag variable $Fg = 0$.

```
if IC(k) == 1 then
    if AMM(k) > AMM_min(k) && Fg == 0 then
        The control objectives are (12);
    else
        The control objectives are (13), and Fg = 1;
    end if
else if IC(k) == 0 && Fg == 1 then
    if The distance between the towing system and the obstacles at time k is larger than that of the time k − 1 then
        The control objectives are (12), and Fg = 0;
    else
        The control objectives are (13);
    end if
else
    The control objectives are (12);
end if
```

Output: Control objectives η_{Sd}, ν_{Sd}.

4.2. MPC-based controller

The core of the MPC strategy is to design the cost function. Based on the control objectives, the cost function of the ship at the time instant k is designed as:

$$J_{\mathrm{S}}(k) = \boldsymbol{e}_{\eta_{\mathrm{S}}}^{\mathrm{T}}(k)\boldsymbol{W}_{\mathrm{S}1}\boldsymbol{e}_{\eta_{\mathrm{S}}}(k) + \boldsymbol{e}_{\nu_{\mathrm{S}}}^{\mathrm{T}}(k)\boldsymbol{W}_{\mathrm{S}2}\boldsymbol{e}_{\nu_{\mathrm{S}}}(k), \tag{14}$$

$$\begin{aligned} \boldsymbol{e}_{\eta_{\mathrm{S}}}(k) &= \boldsymbol{\eta}_{\mathrm{SP}}(k) - \boldsymbol{\eta}_{\mathrm{Sd}}(k) \\ \boldsymbol{e}_{\nu_{\mathrm{S}}}(k) &= \boldsymbol{\nu}_{\mathrm{SP}}(k) - \boldsymbol{\nu}_{\mathrm{Sd}}(k), \end{aligned} \tag{15}$$

where $\boldsymbol{e}_{\eta_{\mathrm{S}}}(k)\in\mathbb{R}^3$ and $\boldsymbol{e}_{\nu_{\mathrm{S}}}(k)\in\mathbb{R}^3$ are the position and velocity error of the ship; $\boldsymbol{\eta}_{\mathrm{SP}}(k)\in\mathbb{R}^3$ and $\boldsymbol{\nu}_{\mathrm{SP}}(k)\in\mathbb{R}^3$ are the predicted position and velocity of the ship; $\boldsymbol{\eta}_{\mathrm{Sd}}(k)\in\mathbb{R}^3$ and $\boldsymbol{\nu}_{\mathrm{Sd}}(k)\in\mathbb{R}^3$ are the desired position and velocity of the ship; $\boldsymbol{W}_{\mathrm{S}1} = diag(w_{\mathrm{Sx}}\ w_{\mathrm{Sy}}\ w_{\mathrm{S}\psi})$ and $\boldsymbol{W}_{\mathrm{S}2} = diag(w_{\mathrm{Su}}\ w_{\mathrm{Sv}}\ w_{\mathrm{Sr}})$ are the weight coefficients.

It is noticed that, there are two parts on the right-hand-side of (14). The first part is the quadratic term of the position error, which is to achieve waypoint following and heading adjusting. The second part is the quadratic term of the velocity error, which is to track the speed profile. When there are no avoiding actions, the second part is the velocity itself, whose role is to restrain the speed of the ship so that the control action of the ship (towing force) is not too aggressive.

For the process of waypoint following, the value of position error at the beginning is maximum, the controller focuses on approaching the waypoint and increasing the ship's speed. As the value of position error reduces, the velocity part is gradually dominant in the cost function, the speed profile-tracking then starts to play the role. Thus, when the avoiding actions have to be taken, to ensure that the speed profile-tracking quickly perform, it is necessary to add a weight factor in the position part to normalize the order of magnitude between the position and velocity errors, and to reduce the sensitivity of the controller to the waypoint distance. The weight factor is designed as a diagonal matrix:

$$\boldsymbol{P}(t) = \begin{bmatrix} 1/d_{\mathrm{W}j}(t) & & \\ & 1/d_{\mathrm{W}j}(t) & \\ & & 1 \end{bmatrix}, \tag{16}$$

$$d_{\mathrm{W}j}(t) = \sqrt{\left(x_{\mathrm{S}}(t) - x_{\mathrm{W}j}\right)^2 + \left(y_{\mathrm{S}}(t) - y_{\mathrm{W}j}\right)^2}, \tag{17}$$

where $d_{\mathrm{W}j}(t)$ is the distance from current position of the ship $(x_{\mathrm{S}}(t), y_{\mathrm{S}}(t))$ to the waypoint j $(x_{\mathrm{W}j}, y_{\mathrm{W}j})$.

Remark (*Weight Factor* $\boldsymbol{P}(t)$)**.** There is no risk that the distance $d_{\mathrm{W}j}(t)$ equals zero, because in the waypoint switch mechanism when the position of the manipulated ship is within a certain range to the waypoint (in the simulation of this paper, this range is set as the half-length of the ship), the controller will treat the current waypoint is achieved, and the desired position of the ship will switch to the next waypoint.

By applying (16) and (17), the cost function in (14) is changed to:

$$J_{\mathrm{S}}(k) = \boldsymbol{e}_{\eta_{\mathrm{S}}}^{\mathrm{T}}(k)\boldsymbol{W}_{\mathrm{S}1}\boldsymbol{P}(k)\boldsymbol{e}_{\eta_{\mathrm{S}}}(k) + \boldsymbol{e}_{\nu_{\mathrm{S}}}^{\mathrm{T}}(k)\boldsymbol{W}_{\mathrm{S}2}\boldsymbol{e}_{\nu_{\mathrm{S}}}(k). \tag{18}$$

The cost function of the tugboat i at the time instant k is designed as:

$$J_i(k) = \boldsymbol{e}_{\eta_i}^{\mathrm{T}}(k)\boldsymbol{W}_{i1}\boldsymbol{e}_{\eta_i}(k) + \boldsymbol{\nu}_{i\mathrm{P}}^{\mathrm{T}}(k)\boldsymbol{W}_{i2}\boldsymbol{\nu}_{i\mathrm{P}}(k), \tag{19}$$

$$\boldsymbol{e}_{\eta_i}(k) = \boldsymbol{\eta}_{i\mathrm{P}}(k) - \boldsymbol{\eta}_{i\mathrm{d}}(k), \tag{20}$$

where $\boldsymbol{e}_{\eta_i}(k)\in\mathbb{R}^3$ is the position error of the tug i; $\boldsymbol{\eta}_{i\mathrm{P}}(k)\in\mathbb{R}^3$ and $\boldsymbol{\nu}_{i\mathrm{P}}(k)\in\mathbb{R}^3$ are the predicted position and velocity of the tug i; $\boldsymbol{W}_{i1} = diag(w_{i\mathrm{x}}\ w_{i\mathrm{y}}\ w_{i\psi})$ and $\boldsymbol{W}_{i2} = diag(w_{i\mathrm{u}}\ w_{i\mathrm{v}}\ w_{i\mathrm{r}})$ are the weight coefficients. The first part on the right-hand-side of (19) is the position error, which is to achieve trajectory tracking for tugboat i. The second part is the velocity of the tugboat i, which is to restrain the speed of the tugboat so that the control action of the tugboat (thruster force) is not too aggressive.

The term $\boldsymbol{\eta}_{i\mathrm{d}}(k)$ is the reference trajectory of the tug i, calculated by:

$$\begin{aligned} \boldsymbol{\eta}_{i\mathrm{d}}(k) = {} & \boldsymbol{\eta}_{\mathrm{SP}}(k) + (l_{\mathrm{tow}i} + l_{\mathrm{T}i})\boldsymbol{E}_i(\psi_{\mathrm{SP}}(k), \alpha_i(k)) \\ & + l_i\boldsymbol{F}_i(\psi_{\mathrm{SP}}(k)) + \alpha_i(k)[0\ 0\ 1]^{\mathrm{T}}, \end{aligned} \tag{21}$$

where $l_{\mathrm{tow}i}$ is the length of the towing line; $\boldsymbol{E}_i\in\mathbb{R}^3$ and $\boldsymbol{F}_i\in\mathbb{R}^3$ are the vectors related to the predicted heading of the ship and the towing angles, formulated as:

$$\begin{aligned} \boldsymbol{E}_i &= (-1)^i \begin{bmatrix} \sin(\psi_{\mathrm{SP}}(k) + \alpha_i(k)) \\ \cos(\psi_{\mathrm{SP}}(k) + \alpha_i(k)) \\ 0 \end{bmatrix} \\ \boldsymbol{F}_i &= (-1)^i \begin{bmatrix} \sin(\psi_{\mathrm{SP}}(k)) \\ \cos(\psi_{\mathrm{SP}}(k)) \\ 0 \end{bmatrix}. \end{aligned} \tag{22}$$

Thus, according to the above cost function, the MPC strategy in the coordination control system can be formulated as:

$$U(k) = \underset{\tau_{\mathrm{S}}\tau_{\mathrm{T}_i}}{\arg\min} \sum_{h=1}^{H_{\mathrm{P}}} \left(w_{\mathrm{S}}J_{\mathrm{S}}(k+h|k) + \sum_{i=1}^{2} w_i J_i(k+h|k) \right) \tag{23}$$

subject to (*i*) The system dynamics,
(*ii*) Operational constraints,

where U are the control inputs of the towing system; w_{S} and w_i are the weight coefficients of the ship and tugboat i; H_{P} is the length of the prediction horizon; h is the hth time prediction step; $J_{\mathrm{S}}(k+h|k)$ and $J_i(k+h|k)$ are the prediction made at k about the cost of the ship and tug i at $k+h$, respectively. The constraints are defined below.

The dynamics of the ship and the tug i are calculated by discretizing the dynamic model in Section 2 (through the Explicit Euler method) with a control sampling time T_s:

$$\begin{aligned}\boldsymbol{\eta}_{SP}(k+1) &= \boldsymbol{\eta}_{SP}(k) + \int_{kT_s}^{(k+1)T_s} \boldsymbol{R}(\psi_S(t))\boldsymbol{\nu}_S(t)dt \\ \boldsymbol{\nu}_{SP}(k+1) &= \boldsymbol{\nu}_{SP}(k) + \int_{kT_s}^{(k+1)T_s} \boldsymbol{M}_S^{-1}[-\boldsymbol{C}_S(\boldsymbol{\nu}_S(t))\boldsymbol{\nu}_S(t) \\ &\quad -\boldsymbol{D}_S\boldsymbol{\nu}_S(t) - \boldsymbol{B}(\alpha_1(t))F_1(t) + \boldsymbol{B}(\alpha_2(t))F_2(t)]dt,\end{aligned} \tag{24}$$

$$\begin{aligned}\boldsymbol{\eta}_{iP}(k+1) &= \boldsymbol{\eta}_{iP}(k) + \int_{kT_s}^{(k+1)T_s} \boldsymbol{R}(\psi_i(t))\boldsymbol{\nu}_i(t)dt \\ \boldsymbol{\nu}_{iP}(k+1) &= \boldsymbol{\nu}_{iP}(k) + \int_{kT_s}^{(k+1)T_s} \boldsymbol{M}_i^{-1}[-\boldsymbol{C}_i(\boldsymbol{\nu}_i(t))\boldsymbol{\nu}_i(t) \\ &\quad -\boldsymbol{D}_i\boldsymbol{\nu}_i(t) + \boldsymbol{B}_i(\beta_i(t))F_i(t) + \boldsymbol{\tau}_{T_i}(t)]dt.\end{aligned} \tag{25}$$

For all k and $i = 1, 2$, the operational constraints for the control inputs are expressed as:

$$-\alpha_{i\max} \le \alpha_i(k) < \alpha_{i\max} \tag{26}$$

$$0 \le F_i(k) \le F_{i\max} \tag{27}$$

$$-\boldsymbol{\tau}_{i\max} \le \boldsymbol{\tau}_i(k) \le \boldsymbol{\tau}_{i\max} \tag{28}$$

$$|\dot{\alpha}_i(k)| \le \bar{\alpha}_i \tag{29}$$

$$\left|\dot{F}_i(k)\right| \le \bar{F}_i \tag{30}$$

where $\alpha_{i\max}$ is the maximum value of towing angle; $F_{i\max}$ is the maximum value of towing force that the two towing lines withstand; $\boldsymbol{\tau}_{i\max}$ is the maximum value of the thruster forces and moment; $\bar{\alpha}_i$ and $\bar{F}_i$ are the maximum change rate value of towing angle and force, respectively.

Constraints (26), (27) and (28) model the saturation of the towing forces, towing angles and thruster forces, stemming from the physical laws and maritime practice [35]; (29) and (30) limit the change rate of the towing angles and forces, in order to make the tug reference trajectory smooth improving the performance of the trajectory tracking.

The MPC-based coordination control scheme is summarized in **Algorithm 2** (at the time instant k).

Algorithm 2 MPC-based Coordination Control Scheme

Input: Control objectives η_{Sd}, ν_{Sd}; Current tug position and velocity $\eta_S(k)$, $\nu_S(k)$, $\eta_i(k)$, $\nu_i(k)$.

1: **if** The control objectives are based on (12) **then**
2: Calculate the optimization problem (23) according to (14), (15), (19) – (22) with the constraints of (24) – (30);
3: **else**
4: Calculate the optimization problem (23) according to (15) – (22) with the constraints of (24) – (30);
5: **end if**

Output: Control inputs of the ship $\tau_S(k)$ and the tugboats τ_{Ti}.

5. Simulation and results

A simulation experiment is carried out in this section for a case study to show the feasibility and applicability of the proposed method adopted for a ship-towing system of small-scale vessels.

5.1. Simulation setup

The operation of towing an unpowered ship is conducted by two tugboats. The model of the two tugs is represented by the "TitoNer" [36], while the towed ship is represented by the "CyberShip II" [37]. The parameters of the towing system can be found in [12].

The parameters of the control system are given in Table 1. In the premises of good visibility conditions, the information for the plan of towing operation is shown in Table 2, which includes the initial states (position and heading) of the ship and two tugboats, the waypoint of the towing system, and the wind speed and direction.

The intruder (target vessel) simulated in this scenario is not under command. Its information is shown in Table 3, including the length and width, the initial position and heading, the average speed, and the turning time.

The detailed simulation results are presented in the next subsection, where they are illustrated in three parts: conflict detection, conflict resolution, and conflict resolution assessment. The first two parts show the performances of the proposed collision avoidance method. The third part evaluates all the potential solutions to provide an optimal collision resolution for the readers.

Table 1
Parameters of the control system.

Control sampling time	$T_s = 1$ s
Prediction horizon	$H_P = 3$
Weight matrices in cost function	$\boldsymbol{W}_{S1} = diag(1 \quad 1 \quad 0.2)$ $\boldsymbol{W}_{S2} = diag(200 \quad 20 \quad 20)$
Weight matrices in cost function	$\boldsymbol{W}_{i1} = diag(1 \quad 1 \quad 1)$ $\boldsymbol{W}_{i2} = diag(2 \quad 2 \quad 2)$
Maximum value of towing angle	$\alpha_{i\max} = 90°$
Maximum value of towing force	$F_{i\max} = 3$ N
Maximum value of the thruster forces and moment	$\tau_{i\max} = [10\text{ N} \quad 10\text{ N} \quad 5\text{ N m}]^T$
Maximum rate of the change of towing angle	$\bar{\alpha}_i = 5°/s$
Maximum rate of the change of towing force	$\bar{F}_i = 0.3$ N/s

Table 2
Information for the plan of towing operation.

Initial States (x(m), y(m), ψ(degree))		
Tug 1	Ship	Tug 2
[-2.17 0 90]	[0 0 90]	[2.08 0 90]
Waypoint (x(m), y(m), ψ(degree))	Wind Information	
	speed (m/s)	Direction (degree)
[50 0 90]	1	225

Table 3
Information of the intruder.

Size of the vessel		Initial Position (x(m), y(m))
Length (m)	Width (m)	
1.255	0.29	(40, -10)
Initial heading (ψ(degree))	Speed (m/s)	Turning Time (s)
330	0.05	The 1st:100 The 2nd: 300.

5.2. Conflict detection and risk assessment

In this phase, conflict detection is the focus of the ship towing system. Fig. 6 shows the changes in the key performance indicators (KPIs) for the risk assessment, and Fig. 7 shows the towing process of the corresponding period.

In Fig. 6, from time 0–130 s, the value of *IC* remains 0 and *AMM* stabilizes at 1, which means in this period there is no collision risk for the ship towing system. At this time instant

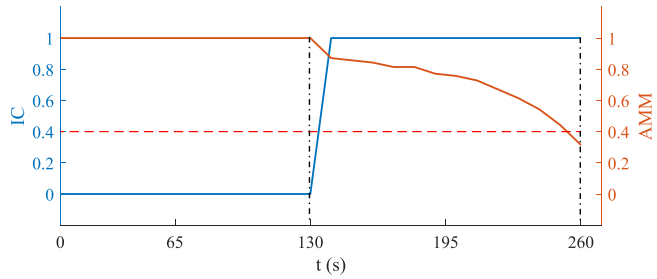

Fig. 6. Key performance indicators (KPIs) of the risk assessment: the blue line stands for the index of conflict *IC*, the orange line represents the available maneuvering *AMM*, the red dashed line is the low threshold of *AMM*. (For interpretation of the references to color in this figure legend, the reader is referred to the web version of this article.)

($t = 130$ s), the position of the towing system and the target vessel are seen in Fig. 7.

After that, the value of *IC* jump to 1 indicating that the collision risk has emerged. Meanwhile, the value of *AMM* starts to reduce, which implies that the situation is getting worse. At $t = 260$ s, the value of *AMM* is already smaller than its low threshold (the red dashed line), the towing system has to take evasive action to eliminate the potential collisions before this moment. Since the frequency of calculating the above two risk KPIs is every 10 s, the time of taking action should be at 250 s.

Besides the position of the towing system, the heading and surge speed of the three vessels can be seen in Fig. 8. It can be seen that under the environmental disturbances, the headings of the three vessels smoothly fluctuate at around 90 degrees, and their surge speeds are around 0.05 m/s. Thus, the above two values are seen as the initial heading and surge speed of the towing system before taking evasive actions in the next phase (conflict resolution).

5.3. Conflict resolution

If the towing system remains at the original heading and speed, collisions will happen. In order to reduce the collision risk, these two states should be changed.

There are four operations for changing the heading and speed of the towing system: Operation I, speed down and port side steering; Operation II, speed down and starboard side steering; Operation III, speed up and port side steering; Operation IV, speed up and starboard side steering. Each operation is simulated in this sub-section to show the collision avoidance performance, where the speed changes are up and down to 20%, and the heading changes are port and starboard side 60 degrees. These operations will last 200 s, if the value of *IC* does not change (remains at the value of 1) over this duration, then it is treated as a failure of resolving the conflict.

Figs. 9 and 10 show the towing process, the risk assessment, and the time-varying heading and speed of the towing system in Operation I (speed down and port side steering). It can be seen that the heading of the controlled towing system changes to 30 degrees. The speed should be controlled to 0.04 m/s, since the towing system is influenced by environmental disturbances, the resulting speed is a little large than this desired value, but it is within the acceptable range. After 80 s (at 330 s), the value of *IC* changes to 0, which means the collision risk is relieved.

Figs. 11 and 12 are the results under Operation II (speed down and starboard side steering). It can be seen that the heading of the

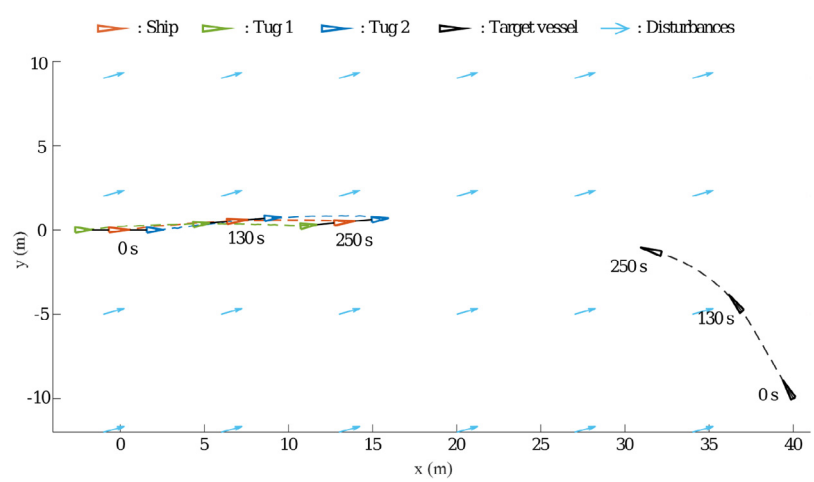

Fig. 7. Towing process in the conflict detection phase.

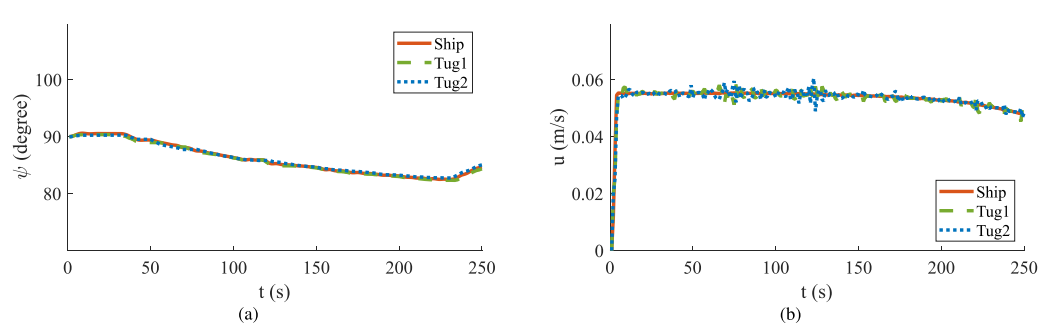

Fig. 8. Time-varying heading and speed of the three vessels in the towing system: (a) Heading; (b) Speed.

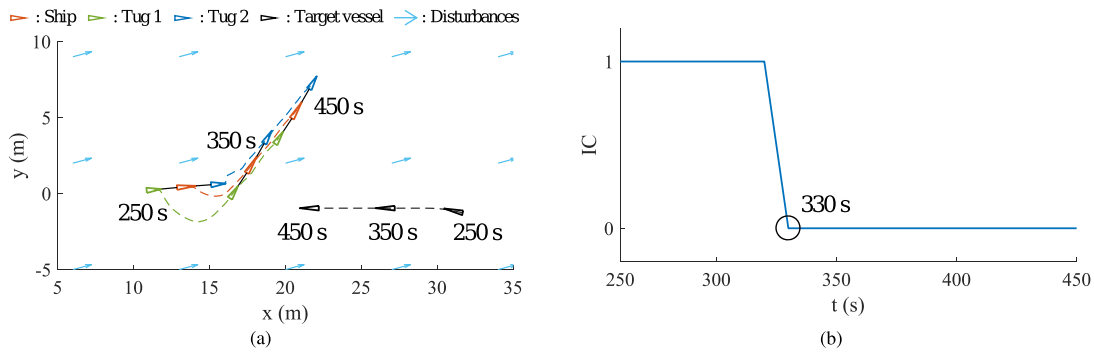

Fig. 9. Towing process and risk assessment of the towing system in Operation I (speed down, port steering): (a) Towing process; (b) Index of conflict.

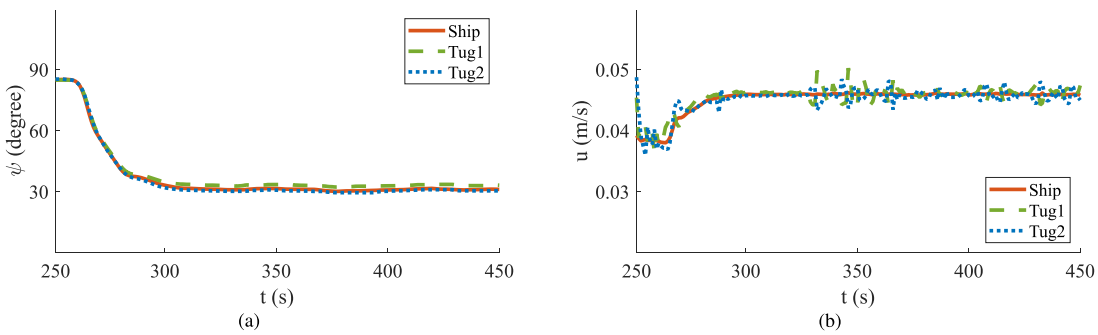

Fig. 10. Time-varying heading and speed of the three vessels in the towing system in Operation I (speed down, port steering): (a) Heading; (b) Speed.

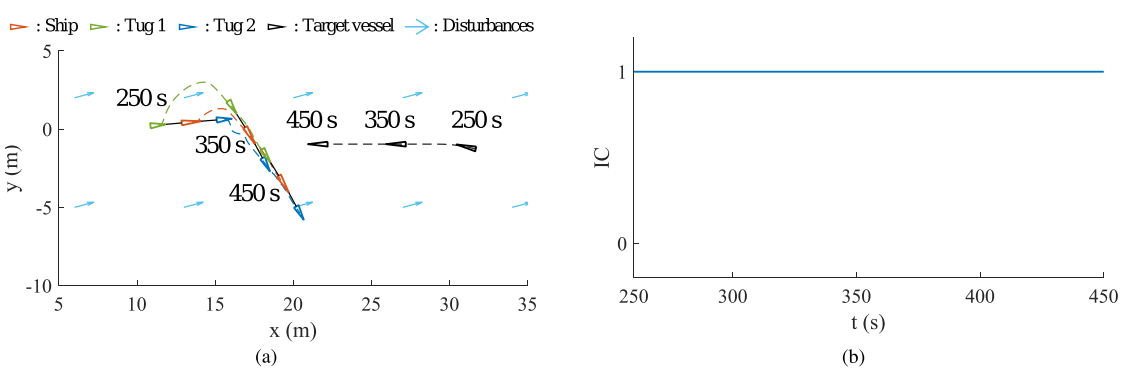

Fig. 11. Towing process and risk assessment of the towing system in Operation II (speed down, starboard steering): (a) Towing process; (b) Index of conflict.

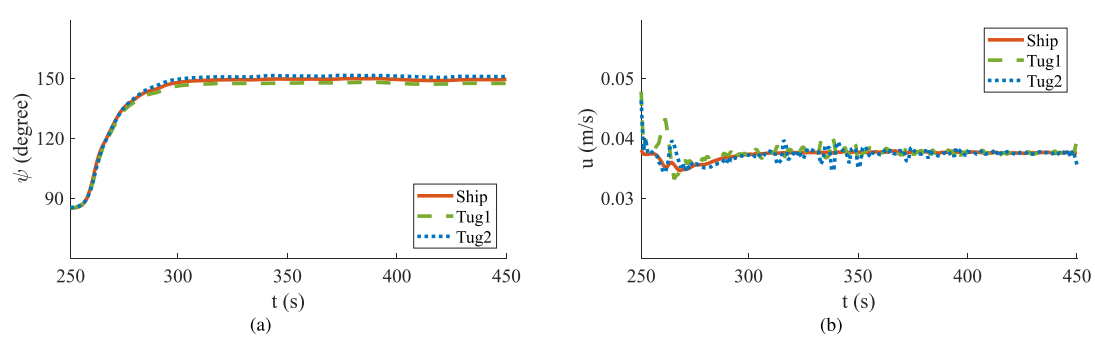

Fig. 12. Time-varying heading and speed of the three vessels in the towing system in Operation II (speed down, starboard steering): (a) Heading; (b) Speed.

controlled towing system changes to 150 degrees, and with the influence of environmental disturbances, its controlled speed is a little smaller than the desired value of 0.04 m/s. As to the KPI of risk assessment, it is noticed that the value of *IC* remains at

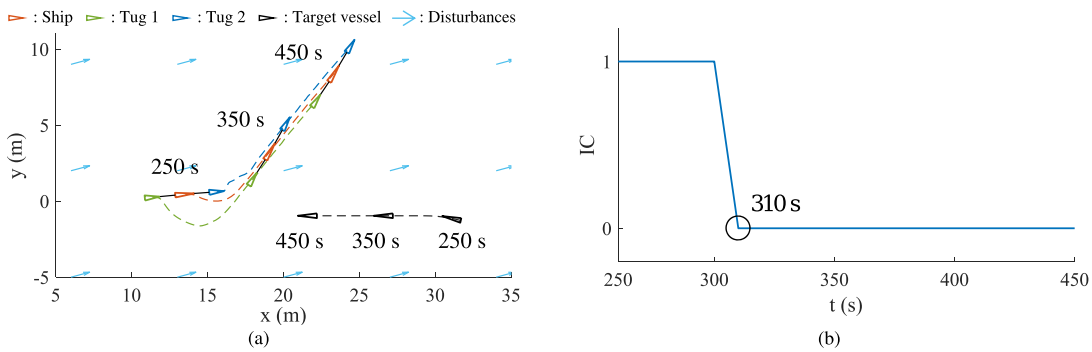

Fig. 13. Towing process and risk assessment of the towing system in Operation III (speed up, port steering): (a) Towing process; (b) Index of conflict.

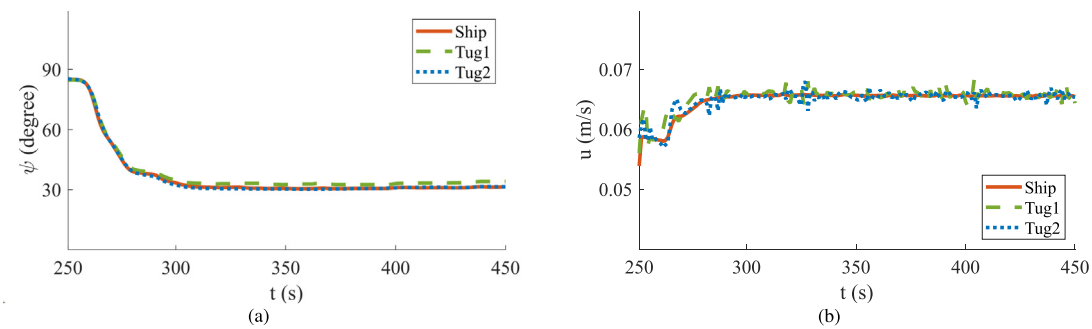

Fig. 14. Time-varying heading and speed of the three vessels in the towing system in Operation III (speed up, port steering): (a) Heading; (b) Speed.

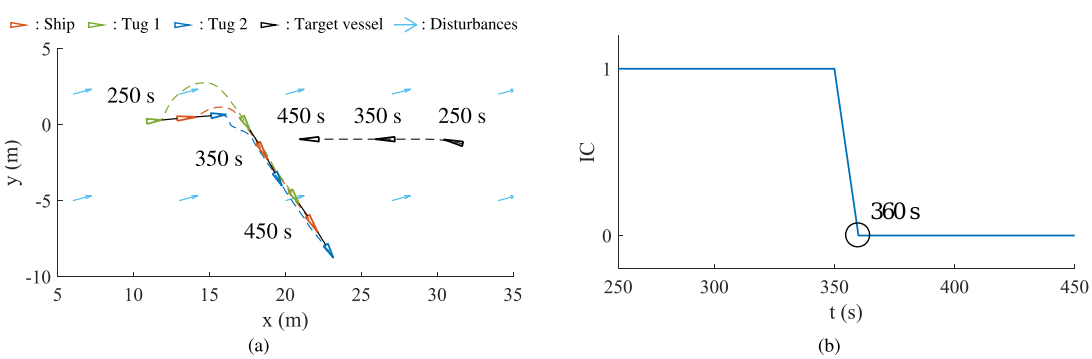

Fig. 15. Towing process and risk assessment of the towing system in Operation IV (speed up, starboard steering): (a) Towing process; (b) Index of conflict.

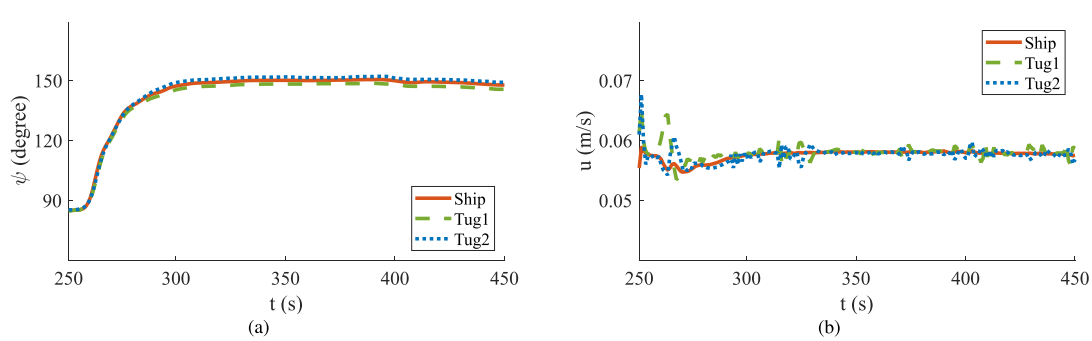

Fig. 16. Time-varying heading and speed of the three vessels in the towing system in Operation IV (speed up, starboard steering): (a) Heading; (b) Speed.

1 till the end. Thus, this example of operation cannot make sure collision avoidance.

The details of Operation III (speed up and port side steering) are shown in Figs. 13 and 14. Besides the similar controlled heading and speed states of the towing system (Fig. 14), it can be seen that the time of resolving the conflict is shorter than the operation of speed down (At time 310 s, the value of *IC* changes to 0). This can be also reflected in the towing process (Fig. 13(a)).

Figs. 15 and 16 are the results for Operation IV (speed up and starboard side steering). Compared to the operation of starboard side steering in Fig. 11, the towing system successfully resolve the conflicts. However, the time cost is much higher than the

Table 4
Conflict resolution time (first one), path returning time (second one), and the fuel consumption (third one) of different avoidance operations (part 1).

Speed	Heading				
	15°	30°	45°	60°	75°
0.01 m/s (−80%)	-	-	-	-	-
0.02 m/s (−60%)	150 s	-	-	-	-
0.03 m/s (−40%)	60 s , 730 s	130 s	-	-	-
0.04 m/s (−20%)	60 s , 700 s	80 s , 660 s	-	-	-
0.05 m/s (Initial)	60 s , 700 s	60 s , 650 s	110 s	190 s	-
0.06 m/s (+20%)	50 s , 660 s	60 s , 610 s	80 s, 570 s, **0.088**	150 s	-
0.07 m/s (+40%)	50 s , 670 s	60 s, 590 s, **0.106**	70 s, 540 s, **0.102**	150 s	-
0.08 m/s (+60%)	50 s , 630 s	60 s, 590 s, **0.128**	70 s, 530 s, **0.124**	150 s	-
0.09 m/s (+80%)	50 s , 620 s	60 s, 580 s, **0.151**	70 s, 510 s, **0.148**	150 s	-
0.10 m/s (+100%)	50 s , 610 s	60 s, 550 s, **0.174**	70 s, 500 s, **0.176**	150 s	-

same speed of port side steering operation (110 s after the initial states).

The computational time in each time step of the four operations is shown in Fig. 17. It can be seen that the main time costs in the four operations are between 0.25 s and 1 s, while the sampling time in the frame of MPC controller is 1 s. So it is possible to apply the proposed control scheme in the real-time controller hardware.

Overall, the results from the above four operational examples indicate that: (*i*) the proposed control scheme can manipulate the ship towing system to achieve the desired heading and speed; (*ii*) the operation of controlling the heading and speed of the ship towing system can relieve the collision risk. However, it is also noticed that the operation of speed down and starboard side steering fails to resolve the conflict. Thus, it is necessary to assess all the potential solutions to check their feasibility and select an optimal one.

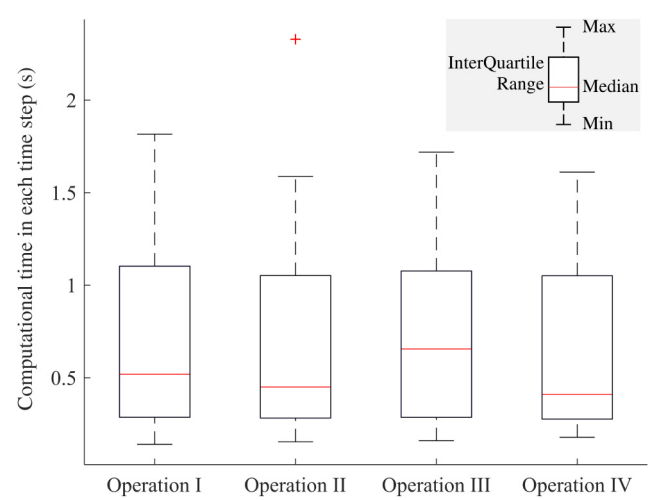

Fig. 17. Computational time in each time step of the four scenarios, the symbol "+" is the outlier.

5.4. Optimal operation selection

In order to select an optimal avoidance operation from all the potential solutions, a set of reachable operations are simulated from the speed of 0.01 m/s (−80%) to 0.1 m/s (+100%) and from the heading of 15° (port steering 75°) to 165° (starboard steering 75°).

There are three criteria for evaluating the solutions: the time of eliminating the risk, the time for returning to the original path, and the fuel consumption of the whole process. The first one is to check whether the conflict is resolved and how long it takes; the second one is based on the first result to calculate the time cost when the towing system returns to its original path; the last one is based on the second results to calculate the fuel consumption of the whole avoidance process.

The results according to the three criteria are presented in Tables 4 and 5. The first value in the cell is the time of eliminating the risk. It can be seen that the possible operations are

Table 5
Conflict resolution time (first one), path returning time (second one), and the fuel consumption (third one) of different avoidance operations (part 2).

Speed	Heading				
	105°	120°	135°	150°	165°
0.01 m/s (−80%)	-	-	-	-	-
0.02 m/s (−60%)	-	-	-	-	-
0.03 m/s (−40%)	-	-	-	-	120 s
0.04 m/s (−20%)	-	-	-	-	70 s, 750 s
0.05 m/s (Initial)	-	-	-	100 s	60 s, 730 s
0.06 m/s (+20%)	-	-	-	110 s	60 s, 670 s
0.07 m/s (+40%)	-	-	-	90 s, 590 s, **0.113**	60 s, 640 s
0.08 m/s (+60%)	-	-	-	70 s, 570 s, **0.133**	60 s, 620 s
0.09 m/s (+80%)	-	-	-	70 s, 540 s, **0.158**	60 s, 660 s
0.10 m/s (+100%)	-	-	140 s	70 s, 530 s, **0.189**	60 s, 630 s

categorized into three parts with different colors: the red cell is the operation that fails to resolve the conflict within 200 s; the blue cell stands for the operation that resolves the conflict with the time between 100 and 200 s; the green one represents the operation that can resolve the conflict within 100 s. The results indicate that for the operation of speed, a proper increasing speed can help to reduce the time of conflict resolution; for the operation of heading, a larger heading change can help resolve the conflict faster (the initial heading is 90 degrees).

After eliminating the collision risk, the time of returning to the original navigation path should be concerned. Figs. 18–20 show the path returning process after resolving the conflict under different speed and heading conflict resolution operations, where the risk is considered relief when every vessel in the towing system has passed the minimum DCPA (Distance at the Closest Point of Approach) to the target vessel. There are four-time instants marked for the ship towing system in these three figures: the first is the initial time of the conflict resolution operation, the second is the time that the index of conflict $IC(t)$ changes from 1 to 0, the third is the time that the towing system is in the minimum DCPA to the target vessel; the fourth is the returning time. It is noticed from the results that the operation of speed up not only costs less time of resolving the conflict but also takes less time for path returning.

In Tables 4 and 5, the second value in the cell is the path returning time, where the standard green cells are the operations with the returning time less than 600 s. The results reveal that the speed-up operation can help a ship towing system quickly resolve conflicts and return to the original path, but as the speed increases to a certain percentage, the rate of time reduction is getting slow. The heading adjusting is another way to solve the conflict: the larger the heading changes, the faster the conflict is solved, but the longer time the towing system returns to its original path.

Finally, the standard green cells are selected to calculate the fuel consumption of the whole collision avoidance process. The calculation is based on the Admiralty coefficient [38], which is defined as:

$$Ac = \frac{\Delta^{2/3} \cdot V^3}{P}, \tag{31}$$

where Δ is the vessel's displacement; V is the vessel's speed; P is the engine break power. Then, the fuel consumption of a vessel during the whole process of collision avoidance can be expressed as [39]:

$$C_{\text{fuel}} = Ac \cdot t_{\text{CA}}, \tag{32}$$

where t_{CA} is the operation time of the collision avoidance.

Since the power source of the ship towing system come from the two tugboats and they have the same model, according to (31) and (32) the fuel consumption in this simulation scenario is determined by the tugboat's speed and the collision avoidance operation time. The results considering fuel consumption in Tables 4 and 5 indicate that the higher speed and the larger heading changes result in higher fuel consumption.

Thus, taking into comprehensive consideration by the conflict resolution time, path returning time, and fuel consumption, the operation of speed up 20% (speed 0.06 m/s) and port side steering

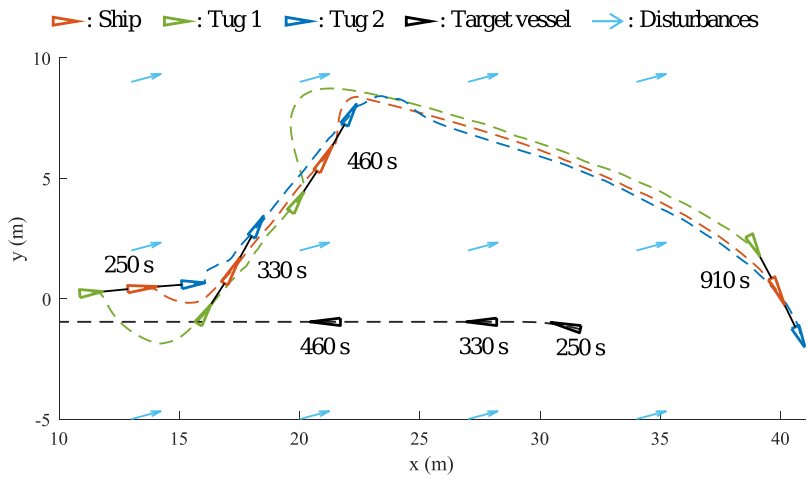

Fig. 18. Path returning process under the conflict resolution operation of speed 0.04 m/s and heading 30°.

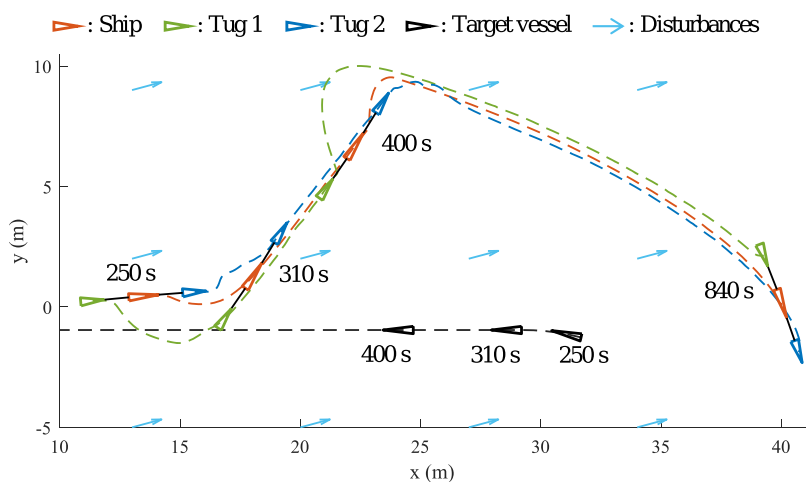

Fig. 19. Path returning process under the conflict resolution operation of speed 0.07 m/s and heading 30°.

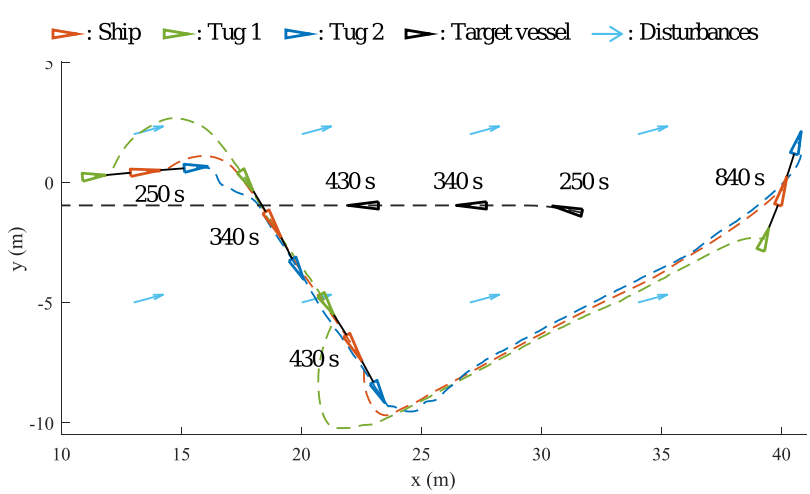

Fig. 20. Path returning process under the conflict resolution operation of speed 0.07 m/s and heading 150°.

45° (heading 45°) is recommended for dealing with collision avoidance for a ship towing system in this simulation scenario (the dark green cell in Table 4).

6. Conclusions

This paper proposes a speed and heading control-based collision avoidance method for a ship towing system. With the foundation of our previous research work on risk alert and detection, this paper focuses on the conflict resolution of the collision avoidance problem.

The conflict resolution for a ship towing system consists of two components: risk assessment and coordination control. The risk assessment identifies the conflict by the calculated index of conflict and determines the time of avoiding action by the available maneuvering margin. The coordination control is based on the model predictive control strategy to cooperatively control two tugboats for regulating the position, heading, and speed of the manipulated ship. To solve the objective conflicts in the optimization control problem, an adaptive weight factor is designed to effectively coordinate the position error and the velocity error in the cost function.

Simulation experiments indicate that: (*i*) The proposed control scheme can manipulate the ship towing system to achieve the desired heading and speed under environmental disturbances; (*ii*) According to the calculated index of conflict and considering the conflict resolution time, path returning time, and fuel consumption, an optimal operation of heading and speed changes can be recommended for a ship towing system to provide a safer and more efficient collision avoidance resolution.

In future research, the following improvements can be made:

1. Calculation of the optimal control objective.
   The control objective decision sub-system in the coordination control system should be redesigned to calculate an optimal control objective for the MPC-based controller. This might be achieved by designing a relationship function that can transform the mentioned criteria into the system states. And then, take advantage of the methods of multi-objective optimization problems [40], to find an optimal reference trajectory and speed profile for the towing system.
2. Implementation of the proposed algorithm.
   In practical implementation, two important issues should be concerned. The first is to consider the time delays in the communication process, which will affect the control performance of the proposed scheme. This issue might be solved by the distributed buffer-based prediction strategy to compensate bounded delays and predict the unavailable states due to delays [41]. Another is to reduce the computation time, which is important for the implementation of the MPC algorithm on real-time hardware. A possible way is to transform the original nonlinear problem into the linear one by linearizing the prediction model and the control constraints [42,43]. The reduction of computation time also helps to extend the prediction horizons, since the short one may lead to instability.

Declaration of competing interest

The authors declare that they have no known competing financial interests or personal relationships that could have appeared to influence the work reported in this paper.

Acknowledgment

This research is supported by the China Scholarship Council under Grant 201806950080.

References

[1] Gu Y, Goez JC, Guajardo M, Wallace SW. Autonomous vessels: state of the art and potential opportunities in logistics. Int Trans Oper Res 2020;28(4):1706–39.
[2] Tam C, Bucknall R, Greig A. Review of collision avoidance and path planning methods for ships in close range encounters. J Navig 2009;62(3):455–76.
[3] Zhao Z, Tang Y, Wu Z, Li Y, Wang Z. Towing analysis of multi-cylinder platform for offshore marginal oil field development. In: Proceedings of the international conference on offshore mechanics and arctic engineering. Busan, South Korea; 2016, V007T06A073.
[4] Mir M, Shafieezadeh M, Heidari MA, Ghadimi N. Application of hybrid forecast engine based intelligent algorithm and feature selection for wind signal prediction. Evol Syst 2019;11(4):559–73. http://dx.doi.org/10.1007/s12530-019-09271-y.
[5] Mirzapour F, Lakzaei M, Varamini G, Teimourian M, Ghadimi N. A new prediction model of battery and wind-solar output in hybrid power system. J Ambient Intell Humaniz Comput 2017;10(1):77–87. http://dx.doi.org/10.1007/s12652-017-0600-7.
[6] Cai W, Mohammaditab R, Fathi G, Wakil K, Ebadi AG, Ghadimi N. Optimal bidding and offering strategies of compressed air energy storage: A hybrid robust-stochastic approach. Renew Energy 2019;143:1–8. http://dx.doi.org/10.1016/j.renene.2019.05.008.
[7] Shigunov V, Schellin TE. Tow forces for emergency towing of containerships. J Offshore Mech Arct Eng 2015;137(5).
[8] Ismail MM, Chalhoub NG, Pilipchuk V. Dynamics and control of a two-ship ensemble connected by a massless towline. Ocean Eng 2021;234:109295.
[9] Banda OAV, Goerlandt F, Kuzmin V, Kujala P, Montewka J. Risk management model of winter navigation operations. Mar Pollut Bull 2016;108(1–2):242–62.
[10] Zhang W, Zou Z, Wang J, Du L. Multi-ship following operation in ice-covered waters with consideration of inter-ship communication. Ocean Eng 2020;210:107545.
[11] Bruzzone G, Bibuli M, Zereik E, Ranieri A, Caccia M. Cooperative adaptive guidance and control paradigm for marine robots in an emergency ship towing scenario. Internat J Adapt Control Signal Process 2016;31(4):562–80.
[12] Du Z, Negenborn RR, Reppa V. Cooperative multi-agent control for autonomous ship towing under environmental disturbances. IEEE/CAA J Autom Sinica 2021;8(8):1365–79.
[13] Liu Z, Zhang Y, Yu X, Yuan C. Unmanned surface vehicles: An overview of developments and challenges. Annu Rev Control 2016;41:71–93.
[14] Huang Y, Chen L, Chen P, Negenborn RR, van Gelder P. Ship collision avoidance methods: State-of-the-art. Saf Sci 2020;121:451–73.
[15] Liu C, Zheng H, Negenborn R, Chu X, Xie S. Adaptive predictive path following control based on least squares support vector machines for underactuated autonomous vessels. Asian J Control 2019;23(1):432–48.
[16] Lazarowska A. A discrete artificial potential field for ship trajectory planning. J Navig 2019;73(1):233–51.
[17] yuan Zhuang J, Zhang L, qi Zhao S, Cao J, Wang B, bing Sun H. Radar-based collision avoidance for unmanned surface vehicles. China Ocean Eng 2016;30(6):867–83.
[18] Huang Y, van Gelder P, Wen Y. Velocity obstacle algorithms for collision prevention at sea. Ocean Eng 2018;151:308–21.
[19] Du Z, Wen Y, Xiao C, Zhang F, Huang L, Zhou C. Motion planning for unmanned surface vehicle based on trajectory unit. Ocean Eng 2018;151:46–56.
[20] Du Z, Wen Y, Xiao C, Huang L, Zhou C, Zhang F. Trajectory-cell based method for the unmanned surface vehicle motion planning. Appl Ocean Res 2019;86:207–21.
[21] Zhu M, Xiao C, Gu S, Du Z, Wen Y. A circle grid-based approach for obstacle avoidance motion planning of unmanned surface vehicles. 2022, arXiv.
[22] Du Z, Negenborn RR, Reppa V. Multi-vessel cooperative speed regulation for ship manipulation in towing scenarios. IFAC-PapersOnLine 2021;54(16):384–9.
[23] Yang Z, Ghadamyari M, Khorramdel H, Alizadeh SMS, Pirouzi S, Milani M, et al. Robust multi-objective optimal design of islanded hybrid system with renewable and diesel sources/stationary and mobile energy storage systems. Renew Sustain Energy Rev 2021;148:111295. http://dx.doi.org/10.1016/j.rser.2021.111295.
[24] Kim H, Kim D, Kim H, Shin J-U, Myung H. An extended any-angle path planning algorithm for maintaining formation of multi-agent jellyfish elimination robot system. Int J Control Autom Syst 2016;14(2):598–607.
[25] Hinostroza M, Xu H, Soares CG. Cooperative operation of autonomous surface vehicles for maintaining formation in complex marine environment. Ocean Eng 2019;183:132–54.
[26] Arrichiello F, Chiaverini S, Fossen T. Formation control of underactuated surface vessels using the null-space-based behavioral control. In: Proceedingsof the 2006 IEEE/RSJ international conference on intelligent robots and systems. Beijing, China; 2006, p. 5942–7.

[27] Qin Z, Lin Z, Yang D, Li P. A task-based hierarchical control strategy for autonomous motion of an unmanned surface vehicle swarm. Appl Ocean Res 2017;65:251–61.
[28] Chen L, Hopman H, Negenborn RR. Distributed model predictive control for vessel train formations of cooperative multi-vessel systems. Transp Res C 2018;92:101–18.
[29] Du Z, Reppa V, Negenborn RR. MPC-based COLREGS compliant collision avoidance for a multi-vessel ship-towing system. In: Proceedings of the 2021 European control conference. Delft, Netherlands; 2021, p. 1857–62.
[30] Fossen TI. Handbook of marine craft hydrodynamics and motion control. Chichester, West Sussex, UK: John Wiley & Sons; 2011.
[31] Huang Y, Gelder P. Non-linear velocity obstacles with applications to the maritime domain. Marit Transp Harvest Sea Resour 2017;999–1007.
[32] Chauvin C, Lardjane S. Decision making and strategies in an interaction situation: Collision avoidance at sea. Transp Res F Traffic Psychol Behav 2008;11(4):259–69.
[33] Du L, Banda OAV, Huang Y, Goerlandt F, Kujala P, Zhang W. An empirical ship domain based on evasive maneuver and perceived collision risk. Reliab Eng Syst Saf 2021;213:107752.
[34] Du L, Banda OAV, Goerlandt F, Kujala P, Zhang W. Improving near miss detection in maritime traffic in the Northern Baltic sea from AIS data. J Mar Sci Eng 2021;9(2):180.
[35] Hensen H. Tug use in port: a practical guide. London, UK: Nautical Institute; 2003.
[36] Haseltalab A, Negenborn RR. Model predictive maneuvering control and energy management for all-electric autonomous ships. Appl Energy 2019;251:113308.
[37] Skjetne R, Smogeli Ø, Fossen TI. Modeling, identification, and adaptive maneuvering of CyberShip II: A complete design with experiments. IFAC Proc Vol 2004;37(10):203–8.
[38] Bialystocki N, Konovessis D. On the estimation of ship's fuel consumption and speed curve: A statistical approach. J Ocean Eng Sci 2016;1(2):157–66.
[39] Kim J-G, Kim H-J, Lee PT-W. Optimizing ship speed to minimize fuel consumption. Transp Lett 2014;6(3):109–17.
[40] Ma Y, Li C, Wang S. Multi-objective energy management strategy for fuel cell hybrid electric vehicle based on stochastic model predictive control. ISA Trans 2022. http://dx.doi.org/10.1016/j.isatra.2022.04.045.
[41] Razavinasab Z, Farsangi MM, Barkhordari M. Robust output feedback distributed model predictive control of networked systems with communication delays in the presence of disturbance. ISA Trans 2018;80:12–21. http://dx.doi.org/10.1016/j.isatra.2018.07.003.
[42] Zheng H, Negenborn RR, Lodewijks G. Predictive path following with arrival time awareness for waterborne AGVs. Transp Res C 2016;70:214–37.
[43] Chen L, Huang Y, Zheng H, Hopman H, Negenborn R. Cooperative multi-vessel systems in Urban waterway networks. IEEE Trans Intell Transp Syst 2020;21(8):3294–307.